eeDAP: An Evaluation Environment for Digital and Analog Pathology

Brandon D. Gallas,[a] Wei-Chung Cheng,[a] Marios A. Gavrielides,[a] Adam Ivansky,[a] Tyler Keay,[a] Adam Wunderlich,[a] Jason Hipp,[b] Stephen M. Hewitt[b]

[a]Division of Imaging and Applied Mathematics, OSEL/CDRH/FDA, Silver Spring, MD

[b]Laboratory of Pathology, Center for Cancer Research, National Cancer Institute, National Institutes of Health, Bethesda, Maryland

ABSTRACT

Purpose: The purpose of this work is to present a platform for designing and executing studies that compare pathologists interpreting histopathology of whole slide images (WSI) on a computer display to pathologists interpreting glass slides on an optical microscope.

Methods: Here we present eeDAP, an evaluation environment for digital and analog pathology. The key element in eeDAP is the registration of the WSI to the glass slide. Registration is accomplished through computer control of the microscope stage and a camera mounted on the microscope that acquires images of the real time microscope view. Registration allows for the evaluation of the same regions of interest (ROIs) in both domains. This can reduce or eliminate disagreements that arise from pathologists interpreting different areas and focuses the comparison on image quality.

Results: We reduced the pathologist interpretation area from an entire glass slide ($\approx$10-30 mm)^2 to small ROIs $<$(50 um)^2. We also made possible the evaluation of individual cells.

Conclusions: We summarize eeDAP's software and hardware and provide calculations and corresponding images of the microscope field of view and the ROIs extracted from the WSIs. These calculations help provide a sense of eeDAP's functionality and operating principles, while the images provide a sense of the look and feel of studies that can be conducted in the digital and analog domains. The eeDAP software can be downloaded from code.google.com (project: eeDAP) as Matlab source or as a precompiled stand-alone license-free application.

Keywords: Digital Pathology, Whole Slide Imaging, Reader Studies, Technology Evaluation

1. INTRODUCTION

Digital pathology (DP) incorporates the acquisition, management and interpretation of pathology information generated from a digitized glass slide. Digital pathology was enabled by recent technological advances in whole slide imaging (WSI) systems, also known as virutal microscopy systems, which can digitize whole slides at microscopic resolution in a short period of time. The potential opportunities with DP are well documented and include telepathology, digital consultation and slide sharing, pathology education, indexing and retrieval of cases, and the use of automated image analysis.[1–3] The imaging chain of a WSI system consists of multiple components including the light source, optics, motorized stage, and sensor for image acquisition. There is also software for auto-focusing, selecting and combining different fields of view in a composite image, and image processing (color management, image compression, etc.). Details regarding the components of WSI systems can be found in Gu et al.[4] There are currently numerous commercially available WSI systems, as reviewed by Rojo et al.[5]

Further author information:
Send Correspondence to BDG. E-mail: brandon.gallas@fda.hhs.gov, Telephone: 2-301-796-2531
Current Affiliation AI: The Institute of Optics, University of Rochester, Rochester, NY
Current Affiliation TK: Omnyx LLC., Pittsburgh, PA

Limited validation studies have been published using WSI, hindering its use in the clinical laboratory. A small number of studies (some cited in Pantanowitz et al. 2013[6]) have focused on validation of whole slide imaging systems for primary diagnosis. A drawback of the above studies is that they combined diagnoses from multiple pathology tasks performed on multiple tissue types. Agreement was typically determined by an adjudication panel comparing pathology reports from the WSI and microscope reads head-to-head. Guidelines were developed for defining major and minor discrepancies, but there is considerable interpretation and judgement required of the adjudication panel as the pathology reports are collected as free text. Another drawback is focus on primary diagnoses, ignoring additional information (finer details and features) used to support a variety of patient management decisions. For example, some additional information obtained from an evaluation of the specimen is used in treatment planning, such as mitotic activity, the status of margins of resection, and tumor grade. In summary, analyses of free text can be subjective and inconsistent, and differences between modalities can be diluted by the pooling of different tasks into one analysis and the focus on primary diagnoses at the expense of finer details and features.

In this paper we present an **e**valuation **e**nvironment for **d**igital and **a**nalog **p**athology that we refer to as **eeDAP**. eeDAP is a software and hardware platform for designing and executing digital and analog pathology studies where evaluation regions of interest (ROIs) in the digital image are registered to the real-time view on the microscope. This registration allows for the reduction or elimination of a large source of variability in comparing these modalities in the hands of the pathologist: the field of view (the tissue) being evaluated. In fact, the current registration precision of eeDAP allows for the presentation of the same individual cell in both domains. As such, a study can be designed where pathologists are asked to evaluate a pre-selected list of individual cells in *Digital mode* and *MicroRT mode* (microscope real-time mode). eeDAP collects the pathologist evaluations while cycling through the list of cells. In *Digital mode*, the pathologist can enter the evaluations himself or herself. In *MicroRT mode*, an administrator enters the evaluations while confirming and maintaining a high level of registation precision. The paired observations allow for comparisons of WSI and traditional optical microscopy using several forms of agreement or performance when a reference standard can be established.

A reader study with eeDAP is intended to evaluate the scanned image, not the workflow of a pathologist or lab. Instead of recording a typical pathology report, eeDAP collects explicit evaluation responses (formatted data) from the pathologist corresponding to very narrow tasks. This approach removes ambiguity related to the range of language and scope that different pathologists use in their reports. At the same time, this approach requires the study designer to narrow the criteria for cases (slides, ROIs, cells) to be included in the study set.

We are currently exploring tasks related to two cell types: mitotic figures (cells undergoing mitosis) and plasma cells. These cell types are part of the pathology evaluation process across many tissue types and diseases. We can formulate many different tasks corresponding to these cell types. Several basic tasks are currently available and customizable in eeDAP: integer input for a scoring or counting task, a slider for a scoring task, check boxes for a classification task, and marking the image for a detection task. We used H&E stained formalin-fixed, paraffin-embedded (FFPE) tissue sections, one of a sarcoma with mitotic figures present, and one of a colonic adenocarcinoma with plasma cells present. We also have images of these slides from a Hamamatsu Nanozoomer 2.0HT at 40x magnification. See Fig. 1 to see examples of the GUI presentation of the scoring task: on the left is colon tissue for identifying plasma cells, on the right is the sarcoma tissue for identifying mitotic figures.

In this paper we outline the key software and hardware elements of eeDAP. First we discuss the software availability and requirements. We next talk about the tone reproduction curves that characterize eeDAP and the native viewers: the curves showing the lightness in the output image given the transmittance of the input slide. In Section 2.3 we summarize the local and global registration methods that are key to pairing ROIs and corresponding evaluations in the digital and microscope domains. In Section 2.4 we provide the key hardware specifications that eeDAP requires and demonstrate the calculation of different fields of view (FOVs) and image sizes. These calculations and representative images help provide a sense of scale across the digital and analog domains. Finally, we talk about reticles and their important role in narrowing the evaluation area to a small ROI or an individual cell.

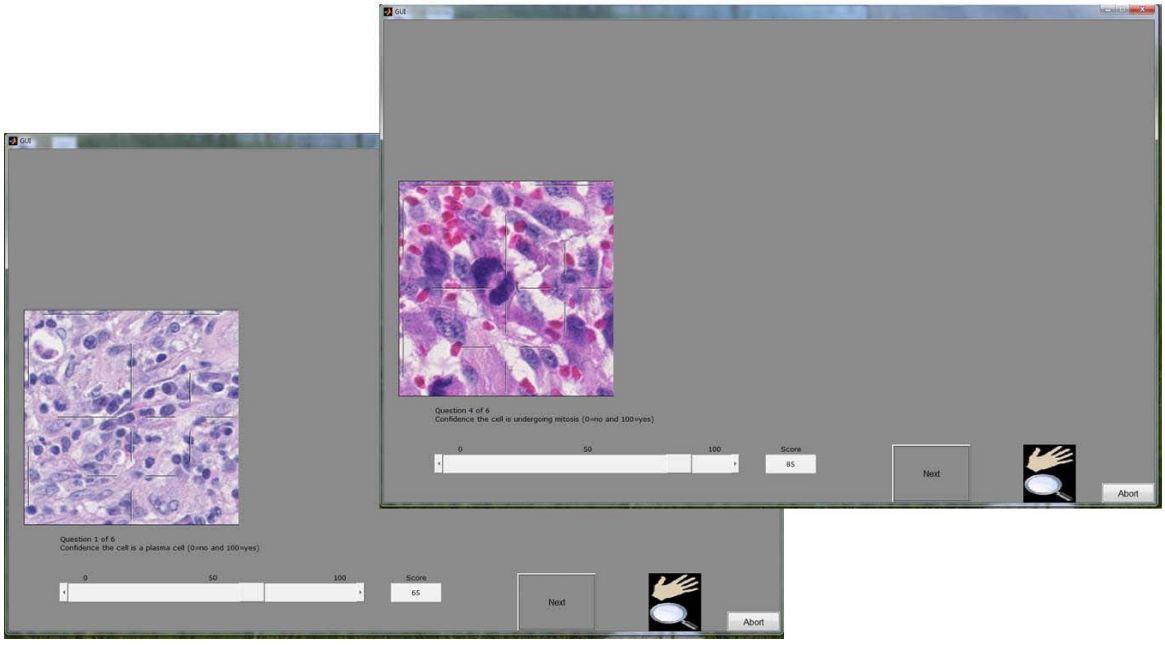

Figure 1. Here are two windows, each showing the eeDAP presentation of a slider task. The image on the left is of colon tissue. The image on the right is of sarcoma tissue.

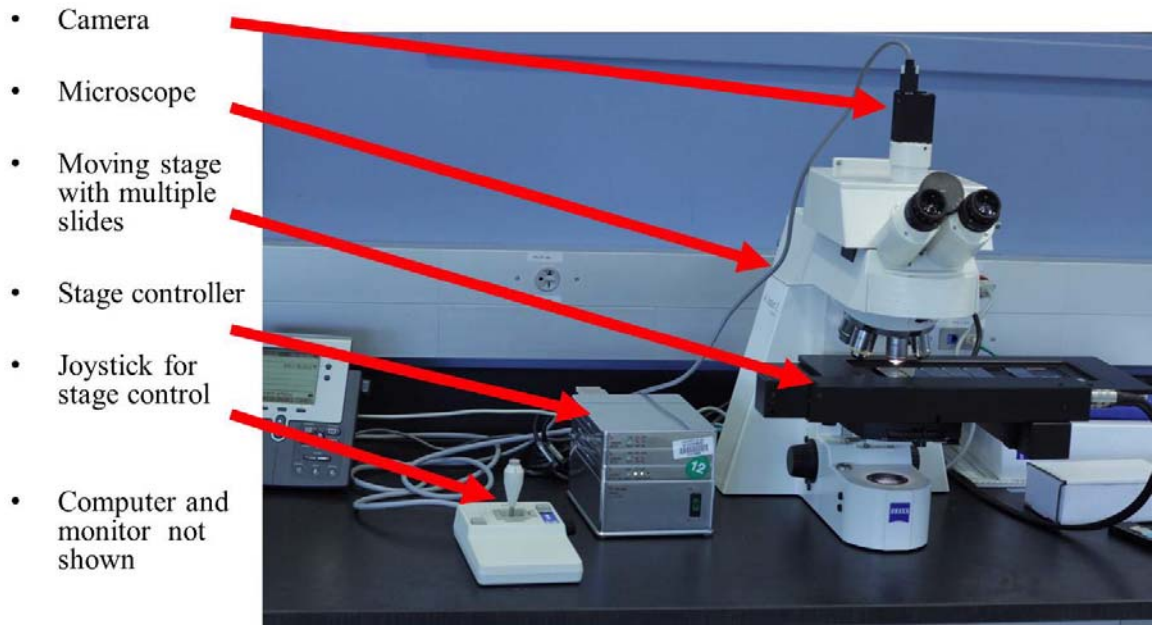

Figure 2. The eeDAP hardware: microscope, camera, computer controlled stage with joystick, and a computer with monitor (not shown).

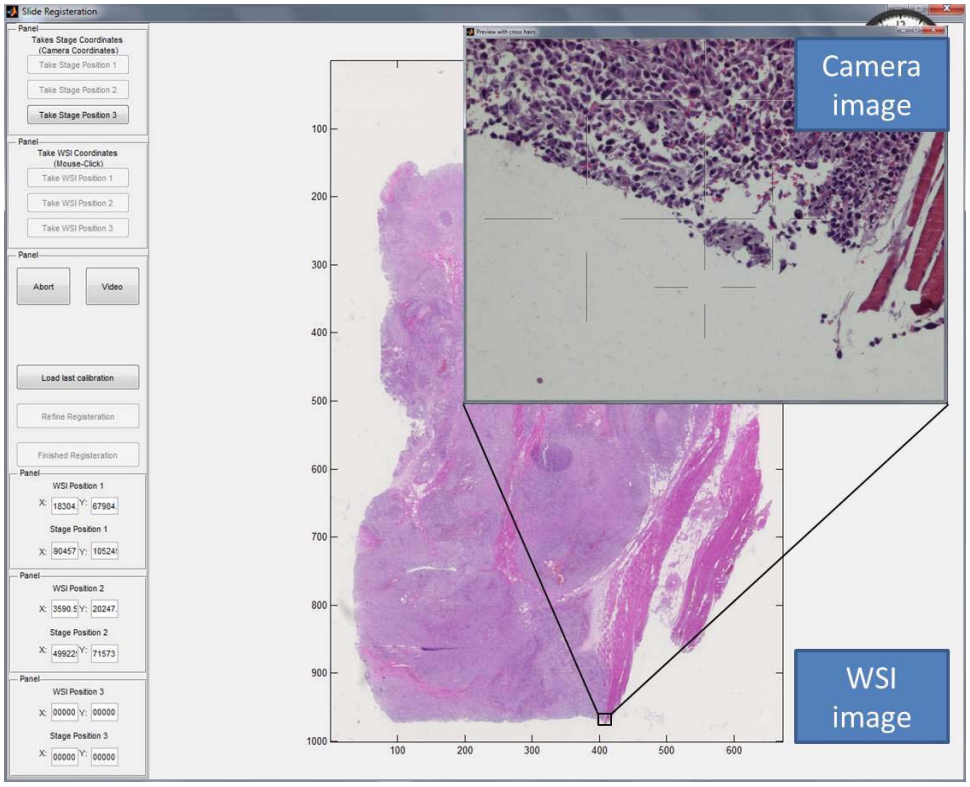

Figure 3. Screen shot of the registration interface including the real-time microscope field of view as seen with the mounted camera ("Preview with cross hairs" window).

2. METHODS

In this section, we summarize the key elements of the eeDAP software and hardware. The eeDAP software is made up of three graphical user interfaces written in Matlab.

The first interface identifies the evaluation mode (*Digital* or *MicroRT*) and the study input file. The input file contains the file names of the WSIs, hardware specifications, and the list of tasks with corresponding ROIs that will be interpreted by the pathologist. Each ROI is defined by a location, width, and height in pixel coordinates of the WSI, and all are automatically extracted on the fly from the WSIs named. In the text that follows we describe installation requirements that make the ROI extraction possible for the proprietary WSI file formats. We also discuss a color comparison between eeDAP and a native WSI viewer (a viewer designed by a WSI scanner manufacturer).

The second interface is executed only if the study is run in *MicroRT mode*. This interface globally registers each WSI to its corresponding glass slide. For each global registration of each WSI, a study administrator must interactively perform three local registrations. The local and global registration methods are described in the text below.

The third interface runs the study defined by the list of tasks given in the input file. If the study is run in the *Digital mode*, the pathologist views the ROIs on the computer display in the GUI and enters the evaluations therein. If the study is run in *MicroRT mode*, the pathologist views the ROIs through the microscope and is responsible for any focusing in the z-plane. While the pathologist is engaged with the microscope, the study administrator is viewing the ROIs on the computer display in the GUI and enters the evaluations therein as dictated by the pathologist. The study administrator is also responsible for confirming and maintaining a high level of registation precision in *MicroRT mode*.

The eeDAP hardware consists of an upright brightfield microscope, a digital camera, a computer-controlled stage with joystick, a computer monitor and a computer (see Fig. 2). Below we summarize how these components are used in registration and how the WSI and real microscope image appear to the pathologist. We also identify an important part of the microscope, the reticle. The reticle is housed in the microscope eyepiece. One reticle that we use identifies ROIs in the microscope field of view and another points at individual cells.

2.1. eeDAP Availability and Requirements

eeDAP is available as Matlab source code or as a precompiled stand-alone license-free application. Simply search code.google.com for the eeDAP project site to find and download the source or the application and a user manual.

Running eeDAP source code requires the Matlab Image processing toolbox and installation of third party software to extract ROIs from WSIs. WSIs are often extremely large (several GB) and are stored as large layered TIFF files embedded in proprietary WSI file formats. eeDAP uses ImageScope, a product of Aperio (a Leica Biosystems Division) to read images scanned with WSI scanners from Aperio (.svs) and other formats, including .ndpi (Hamamatsu). ImageScope contains an ActiveX control named TIFFcomp that allows for the extraction and scaling of ROIs. A consequence of using TIFFcomp is that the Matlab verion must be 32-bit.

The precompiled stand-alone application also requires that the Matlab compiler runtime (MCR) library be installed. It is important that the version of the MCR correspond exactly to that used for the stand-alone application (refer to the user manual).

eeDAP currently supports a Ludl controller and compatible xy stage, an IEEE 1394 "FireWire" camera communicating according to a DCAM interface, and selected reticles (See Sect. 2.5). Set-up instructions and example specifications can be found in the user manual.

2.2. Tone Reproduction Curves

Manufacturers of WSI scanners typically provide software for viewing their proprietary WSI file formats. These viewers may perform specialized color management. In fact, we observed color differences when we viewed .ndpi images with the native Hamamatsu viewer (NDP.View) side-by-side with the Aperio viewer (ImageScope) and Matlab (with the Aperio ImageScope Active X component FTIFFcomp). In an attempt to correct for these differences, we considered the image adjustments possible. Of these, we observed that the images appeared the same in the three viewers when we adjusted the gamma setting. To confirm our observations, we measured the tone reproduction curves of NDP.view (gamma = 1.8 and gamma = 1.0) and ImageScope (no adjustments made).

Following the work of Cheng et al. 2013[7] we measured the transmittance of the 42 color patches of a color phantom (film on a glass slide, see Fig. 4). Using an FPGA board, we then retrieved the sRGB values of a Hamamatsu scanned image of the color phantom from NDP.view with gamma set to 1.8 (default), gamma set to 1.0 (turning off the gamma adjustment), and ImageScope (no gamma correction). We then converted the sRGB values to the CIELAB color space and plotted the normalized lightness L* against the normalized transmittance. The results supported our visual observations:

- There is good agreement between the tone reproduction curves of NDP.view with gamma=1.0 and ImageScope
- The tone reproduction curve of NDP.view with gamma=1.0 appears to be linearly related to transmittance.
- The tone reproduction curve of NDP.view with gamma=1.8 appears to be 1/1.8 gamma transformation of transmittance.

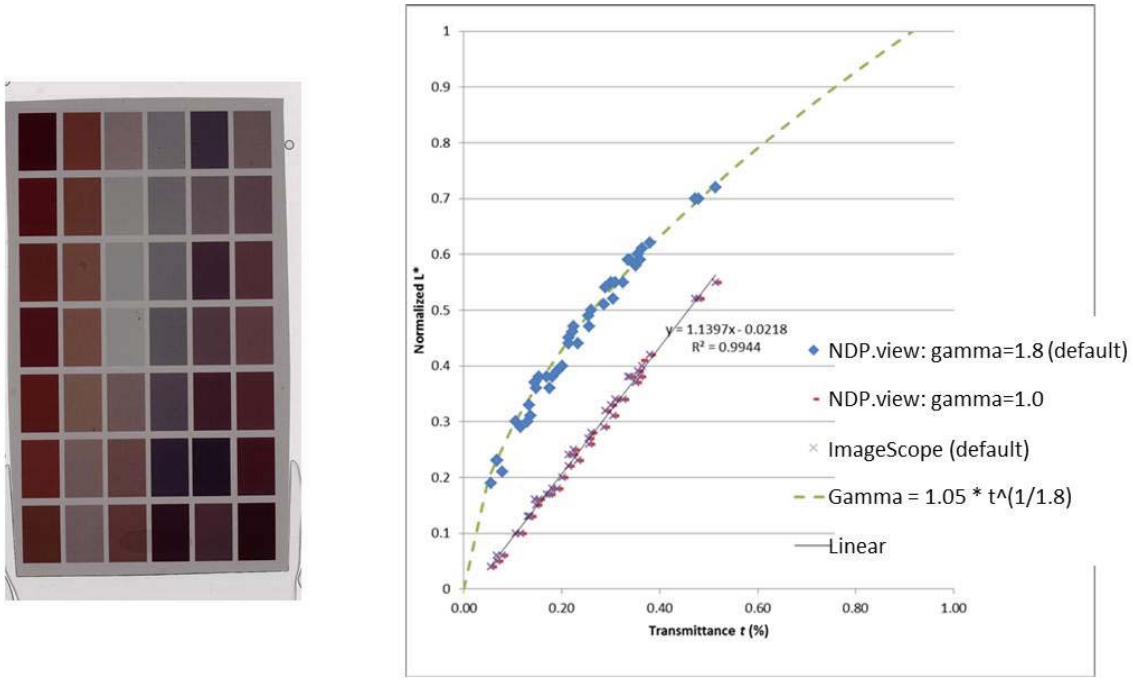

Figure 4. Left: Hamamatsu scanned image of a color phantom (film on a glass slide). Right: The transmittance of the 42 color patches plotted against the normalized lightness L* in the CIELAB color space (derived from the average sRGB values in a patch).

2.3. Registration

eeDAP uses registration to link the stage (glass slide) coordinates to the WSI coordinates. eeDAP has two levels of registration: global and local. The global registration is equivalent to finding the *transformation* between the stage and WSI coordinates. The global registration requires three anchors, three pairs of stage-WSI registered coordinates. Each anchor is generated by a local registration and corresponds to an (x, y) stage coordinate and an (x, y) WSI coordinate that correspond to the same specimen location.

eeDAP conducts two levels of Global registration: low and high resolution. Low resolution corresponds to microscope magnifications such as 2x, 5x, and 10x; the entire WSI image is scaled to fit in the graphical user interface. High resolution registration corresponds to microscope magnifications such as 20x and 40x; the low-registration results are used to limit the amount of the WSI shown in the graphical user interface, apparently zooming in on the location of the anchor.

eeDAP uses local registration for two purposes. The first purpose is to support global registration as discussed. The second purpose is to maintain a high level of registration precision throughout data collection. During our pilot studies we observed that the precision of the stage motion was not as good as our registration precision. Therefore, we implemented a button that could be pressed during data collection that could register the current microscope view to the current task-specific ROI. The current level of precision appears to allow for the reliable evaluation of individual cells.

2.3.1. Local Registration

A local registration is accomplished by taking a snapshot of the microscope field of view with the camera and by finding a search region containing the corresponding location in the WSI (see Fig. 3). The search region is identified by the study administrator and avoids searching the entire (very large) image. A local registration yields an (x, y) coordinate in the WSI and an (x, y) coordinate on the microscope stage.

The camera image contains some amount of the specimen on the glass slide and is labeled by the (x, y) coordinate of the current stage position. See for example the "Preview with cross hairs" window labeled "Camera image" depicted in Fig. 3. The camera image has three channels (RGB) and must be at least 640×480. The physical size of a camera pixel is given by the manufacturer specifications (the camera pixels are square so size equals length equals width). This size and any magnification by the microscope (objective × camera adapter) are inputs to eeDAP and determine how much of the specimen each pixel captures.

We extract a patch of the WSI image (RGB) that is larger than and contains the same content as captured by the camera. See for example the image labeled "WSI image" depicted in Fig. 3. The size of a WSI pixel is given by the manufacturer specifications in units of the specimen and is often recorded in the WSI image. This size is also an input to eeDAP and determines the size of WSI patches in units of the specimen. The size of a WSI image is rescaled (interpolated) such that the pixels have the same size as the camera image using the ratio of the size of a scanner pixel to that of a camera pixel. In other words

$$\left[\begin{array}{c}\text{rescaled}\\ \text{size of WSI image}\end{array}\right] = \frac{\text{size of WSI pixel}}{\text{size of camera pixel}} \left[\begin{array}{c}\text{unscaled}\\ \text{size of WSI image}\end{array}\right]. \tag{1}$$

Given the camera image $c(x, y)$ and the WSI image $d(x, y)$ at the same scale, we perform normalized cross-correlation to find the $\Delta x, \Delta y$ shift that best registers the two images. In other words we find $\Delta x, \Delta y$ that maximize the following sum

$$\frac{1}{n} \sum_{x,y} \frac{(c(x, y) - \overline{c}) \left(d(x + \Delta x, y + \Delta y) - \overline{d}\right)}{\sigma_c \sigma_d}, \tag{2}$$

where the sum is over the n pixels in the camera image, (x, y) index the pixels in the image, $\Delta x, \Delta y$ is the shift in pixels, and $\overline{c}, \sigma_c$ and $\overline{d}, \sigma_d$ are the average and standard deviation of the elements of $c(x, y)$ and $d(x, y)$ considered in the sum.

2.3.2. Global Registration

Global registration is done for each WSI in the input file. Each global registration is built on three local registrations. The three local registrations yield three pairs of coordinates that define the transformation (the change of basis) between the coordinate system of the WSI (image pixels) and the coordinate system of the stage (stage pixels).

Let the three pairs of coordinates be given by $\left(x_i^{WSI}, y_i^{WSI}\right)$, $\left(x_i^{stage}, y_i^{stage}\right)$ for $i = 1, 2, 3$. Given these pairs we define the two coordinate systems with the following matrices

$$M_{WSI} = \left[\begin{array}{cc} x_2^{WSI} - x_1^{WSI}, & x_3^{WSI} - x_1^{WSI} \\ y_2^{WSI} - y_1^{WSI}, & y_3^{WSI} - y_1^{WSI} \end{array}\right], \tag{3}$$

$$M_{stage} = \left[\begin{array}{cc} x_2^{stage} - x_1^{stage}, & x_3^{stage} - x_1^{stage} \\ y_2^{stage} - y_1^{stage}, & y_3^{stage} - y_1^{stage} \end{array}\right]. \tag{4}$$

Then given a new location in the WSI coordinate system $\left[x_{new}^{WSI}, y_{new}^{WSI}\right]^t$, we can determine the corresponding location in the stage coordinate system with the following transformation:

$$\left[\begin{array}{c} x_{new}^{stage} \\ y_{new}^{stage} \end{array}\right] = M_{stage} M_{WSI}^{-1} \left(\left[\begin{array}{c} x_{new}^{WSI} \\ y_{new}^{WSI} \end{array}\right] - \left[\begin{array}{c} x_1^{WSI} \\ y_1^{WSI} \end{array}\right] \right) + \left[\begin{array}{c} x_1^{stage} \\ y_1^{stage} \end{array}\right]. \tag{5}$$

In words, we first shift the new point according to the origin in the WSI coordinate system $\left(x_1^{WSI}, y_1^{WSI}\right)$. Next, we map the point from the WSI coordinate system to the standard one with M_{WSI}^{-1} and then map it to the stage coordinate system with M_{stage}. Finally, we shift the point according to the origin in the stage coordinate system $\left(x_1^{stage}, y_1^{stage}\right)$. Consequently the location of each ROI for each task given in the input file can be accessed in the WSI coordinate system or the stage coordinate system.

The study administrator determines each local registration by navigating the microscope with the joystick to an appropriate anchor, taking the camera image, and then approximately identifying the corresponding anchor

in the WSI. An appropriate anchor is one that can be recognized in the WSI image and is surrounded by one or more unique features. Unique features increase the likelihood of a successful registration; repetitive features and homogeneous regions do not.

In Fig. 3 we see the camera image and the digital image. The study administrator has clicked on the digital image to produce the blue rectangle, which represents the size of the camera, and the red rectangle, which is twice as big. The number 3 is also shown to indicate the third anchor. If the study administrator is satisfied that the red rectangle includes the region captured in the camera image, an equivalent patch is extracted from the WSI at the full scanning resolution, the patch is scaled to the resolution of the camera, and a local registration produces the shift that identifies the corresponding WSI location to pair with the current stage location.

Determining the anchors is not challenging or highly critical. The set of three anchors should be as widely separated as possible for a successful global registration. The most challenging aspect to finding appropriate anchors is navigating the microscope stage with the joystick, focusing on the specimen, and determining the corresponding location in the WSI image.

2.4. Comparing Fields of View and Image Sizes

In the following we provide the key hardware specifications that eeDAP requires and demonstrate the calculation of different fields of view (FOVs) and image sizes. These calculations help provide a sense of scale across the digital and analog domains.

2.4.1. Microscope FOV

An important parameter of an optical microscope is the field number (FN); it is the diameter of the view field in milimeters at the intermediate image plane, which is located in the eyepiece. The FN is a function of the entire light path of the microscope after the objective and before the eyepiece, and is often inscribed on the eyepiece. To get the FOV in units of the specimen being viewed, we divide the FN by the objective magnification. We currently have an Olympus BX43 microscope (FN=22 mm) and a Zeiss Axioplan2 Imaging microscope (FN=23 mm). At 40x magnification due to the objective, the FOV covered in the specimen plane is given by

- diameter = 0.550 mm (22/40), area = 0.2376 mm^2 (Olympus FOV at 40x)
- diameter = 0.575 mm (23/40), area = 0.2597 mm^2 (Zeiss FOV at 40x).

The FN can also be used to determine perceived size of the microscope image at an effective viewing distance of 25 cm. The 25 cm effective viewing distance is a design convention[8] that is not well documented or known. The perceived size is then simply the FN times the eyepiece magnification. Since the eyepieces on both microscopes above have 10x magnfication, the perceived diameters of the intermediate images are then 22 cm (Olympus) and 23 cm (Zeiss) at the effective viewing distance of 25 cm (area$\approx$380 cm^2). This corresponds to a visual angle (subtended angle of object at the eye) equal to $2 \times \arctan(23/(2 * 25)) \approx 50°$. In Fig. 5 we show what the microscope FOV looks like for the sarcoma slide scaled to fit the page.

2.4.2. Size of Scanner Images

We have access to two WSI scanners: a Hamamatsu Nanozoomer 2.0HT and an Aperio CS. They both operate at 20x and 40x magnification equivalent settings with similar pixel sizes:

- 0.4558 um at 20x and 0.2279 um at 40x (Hamamatsu);
- 0.5000 um at 20x and 0.2500 um at 40x (Aperio).

The 40x Hamamatsu scanned images we have been using for pilot studies have 123,008×82,688 pixels and 39,680×51,200 pixels. By multiplying the number of pixels by the size of the pixels, we get the size of the images in units of the specimen on the glass slide. These images correspond to image areas of 28.0 mm×18.8 mm and 9.0 mm×11.7 mm. We have been extracting 400x400 ROI patches that show 0.092 mm×0.092 mm patches of the specimen (area$\approx$0.0084 mm^2) for our most recent pilot study, which is 3.2% of the microscope FOV.

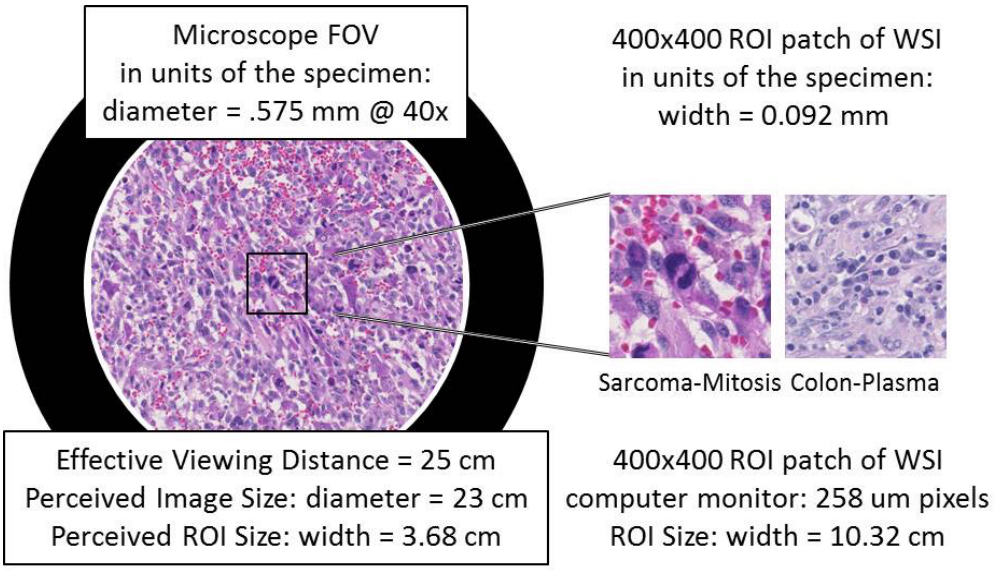

Figure 5. The two images in this figure depict the relative sizes of the microscope image as seen through the eyepiece at 40x (left) and a 400x400 ROI patch from a WSI as seen on a computer monitor with 258 um pixels at a viewing distance of 25 cm (right).

The size of a patch seen by a pathologist depends on the computer monitor pixel pitch (distance between pixels). For a computer monitor with 258 um pixel pitch, the display size of a 400x400 patch is 10.32 cm×10.32 cm (area≈106 cm^2). If we assume a viewing distance of 25 cm from the computer monitor to match the effective viewing distance in the microscope, we can compare the image size of the ROI on the computer monitor to the microscope preceived image size. We show the relative sizes of the two views side by side in Fig. 5. This figure allows us to appreciate the apparent magnification of the specimen area in the displayed 400x400 patch,

2.4.3. Size of Camera Images

We currently have a Point Grey Flea2 color camera (FL2G-50S5C-C) that has a default output format of 1024×768 with 6.9 um pixels. This format corresponds to 2×2 binning of a camera with native pixel size of 3.45 um. At 20x magnification (40x objective times 0.5x camera adapter), the pixel size corresponds to 0.345 um (6.9/20) and the camera field of view is 0.353 mm×0.265 mm (area=0.0234 mm^2), which is about 36% of the microscope FOV.

2.5. Reticles

Reticles are pieces of glass that are inserted at the intermediate image plane in the eyepiece. They contain fine lines and grids that appear superimposed on the specimen. Reticles help measure features or help locate objects. eeDAP uses them to narrow tasks to very small regions and individual cells. In Fig. 6 we depict reticles as seen through the microscope (line thickness exaggerated) and as they appear in eeDAP (400x400 patches). These reticles are described below.

We have conducted a pilot study with a reticle containing a 10x10 grid with squares that are 1.25 mm on a side (Klarmann Rulings: KR-429). At 40x these squares are 31.25 um on a side in the specimen plane. When running in *Digital mode*, eeDAP digitally creates a reticle mask to create the same effect as the real reticle in the microscope. The instructions for this study were to score the reticle square that was immediately above and to the right of the center cross (red squares in Fig. 6). Identifying the center cross in the 10x10 grid in *MicroRT mode* could be challenging. It could be accomplished by rotating the eyepiece, as the center cross remains fixed. Additionally, the instructions to score a square were to score the cell that was most likely the target (mitotic figure or plasma cell), considering cells with at least half their nuclei in the square.

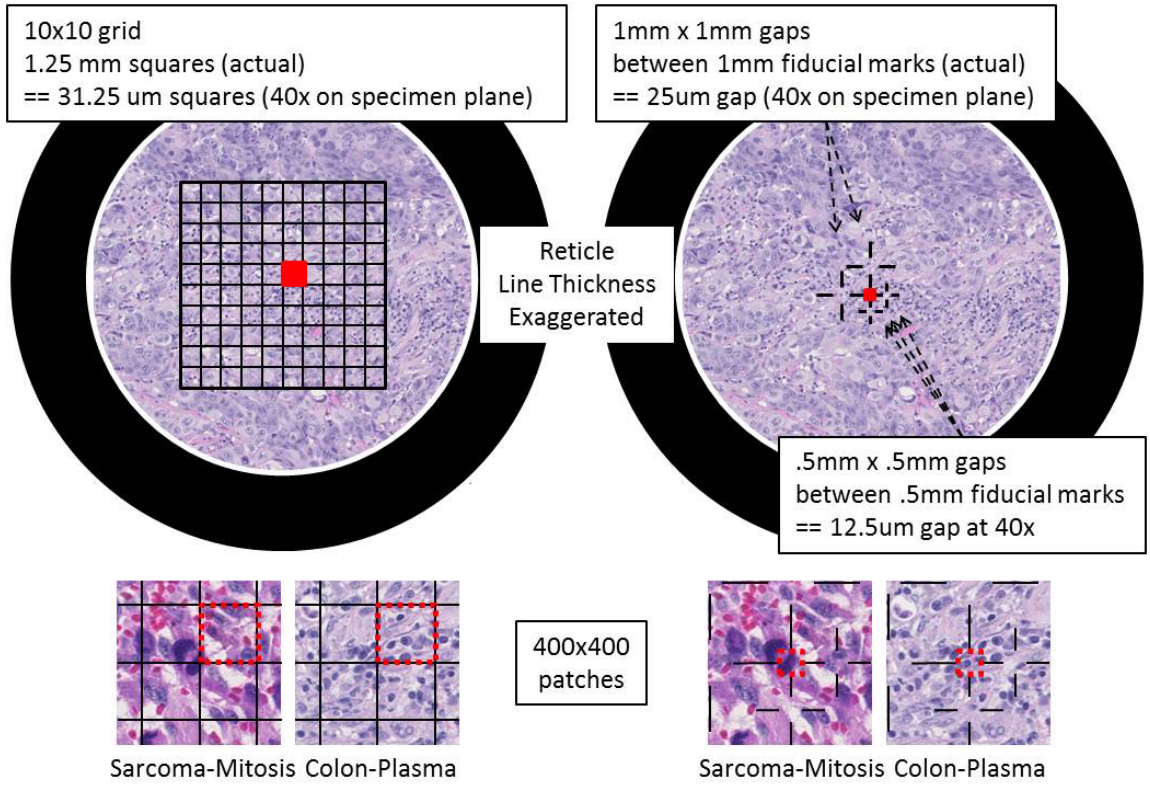

Figure 6. Reticles as seen through the microscope (line thickness exaggerated) and as they appear in eeDAP (400x400 patches).

Another pilot study was conducted with a custom reticle that has fiducials that point to gaps (Klarmann Rulings: KR-32536). Two gaps are 1 mm×1 mm and three gaps are 0.5 mm×0.5mm. At 40x these gaps are 25.0 um and 12.5 um on a side. The instructions for this study were much more direct: score the cell at the center of the center fiducials (red squares in Fig. 6).

3. SUMMARY

In this paper we presented the key software and hardware elements of eeDAP. The software part of eeDAP can be downloaded from code.google.com (project: eeDAP), paired with the required hardware (microscope, automated stage, and camera), and used to design and execute reader studies to compare digital pathology to traditional optical microscopy.

We have been using pilot studies to identify weaknesses and needs from eeDAP and the general study design. The main weakness that we identified was that the registration precision throughout data collection was not good enough: pathologists were not evaluating identical ROIs. We have addressed this in the current generation of eeDAP by incorporating a local registration for every task-specific ROI during data collection. We have also created a custom reticle that allows us to point at individual cells. This reduces ambiguity and disagreements due to evaluations based on multiple different cells within an ROI.

We also observed that the .ndpi WSI images appeared darker when viewing with eeDAP (and ImageScope) compared to viewing with the native viewer, NDP.view. Through observation and subsequent measurement, we determined that the difference was a simple gamma adjustment, and we implemented a color look-up-table to make this and any other color adjustment possible with eeDAP.

Other weaknesses identified during the pilot studies are related to training. Consequently, we are focusing our efforts to creating training on the cell types and scoring. Training on cell types may include power point slides that contain verbal descriptions of typical features and sample images. Training may also include eeDAP training modules: the training modules may elicit scores of the typical features as well as the overal score and then provide feedback from an expert on the score of the typical features and the overall score.

As we move beyond pilot studies to pivotal studies we need to investigate and establish many methods and protocols on issues such as

- computer monitor QA/QC and calibration,
- microscope and camera calibration,
- slide preparation, and
- tissue inclusion/exclusion criteria, including methods to objectively identify target cells for the evaluation task.

Finally, a coherent analysis method is needed that does not require a gold standard, since one is typically not available for the tasks being considered. To address this need we are investigating agreement measures, such as concordance, that compare pathologist performance with WSI to conventional optical microscopy. The goal is to develop methods and tools for multi-reader, multi-case analysis of agreement measures, similar to the methods and tools for the area under the ROC curve.[9]

Acknowledgements

This research project was partially funded through a Critical Path grant from the U.S. Food and Drug Administration (FDA/CDRH). We would like to acknowledge Catherine Conway, formerly at the NIH, for her active involvement in the project, including the preparation and annotation of slides and training materials.

The mention of commercial entities, or commercial products, their sources, or their use in connection with material reported herein is not to be construed as either an actual or implied endorsement of such entities or products by the Department of Health and Human Services or the U.S. Food and Drug Administration.

REFERENCES

1. Pantanowitz, L., Valenstein, P. N., Evans, A. J., Kaplan, K. J., Pfeifer, J. D., Wilbur, D. C., Collins, L. C., and Colgan, T. J., "Review of the current state of whole slide imaging in pathology.," *J Pathol Inform* **2**, 36 (2011).
2. Weinstein, R. S., Graham, A. R., Richter, L. C., Barker, G. P., Krupinski, E. A., Lopez, A. M., Erps, K. A., Bhattacharyya, A. K., Yagi, Y., and Gilbertson, J. R., "Overview of telepathology, virtual microscopy, and whole slide imaging: prospects for the future.," *Hum Pathol* **40**, 1057–1069 (Aug 2009).
3. Al-Janabi, S., Huisman, A., and Van Diest, P. J., "Digital pathology: current status and future perspectives.," *Histopathology* **61**, 1–9 (Jul 2012).
4. Ogilvie, R. W., [*Virtual microscopy and virtual slides in teaching, diagnosis, and research*], CRC Press, Boca Raton, FL (2005).
5. Rojo, M. G., García, G. B., Mateos, C. P., García, J. G., and Vicente, M. C., "Critical comparison of 31 commercially available digital slide systems in pathology.," *Int J Surg Pathol* **14**, 285–305 (Oct 2006).
6. Pantanowitz, L., Sinard, J. H., Henricks, W. H., Fatheree, L. A., Carter, A. B., Contis, L., Beckwith, B. A., Evans, A. J., Lal, A., and Parwani, A. V., "Validating whole slide imaging for diagnostic purposes in pathology: guideline from the college of american pathologists pathology and laboratory quality center.," *Arch Pathol Lab Med* **137**, 1710–1722 (Dec 2013).
7. Cheng, W.-C., Keay, T., O'Flaherty, N., Wang, J., Ivansky, A., Gavrielides, M. A., Gallas, B. D., and Badano, A., "Assessing color reproducibility of whole-slide imaging scanners," in [*Medical Imaging 2013: Digital Pathology*], Gurcan, M. N. and Madabhushi, A., eds., *Proc SPIE* **8676-23** (2013).

8. Kapitza, H. G., *Microscopy from the very beginning.* Carl Zeiss, 2nd ed. (1997).
9. Gallas, B. D., Bandos, A., Samuelson, F., and Wagner, R. F., "A framework for random-effects ROC analysis: Biases with the bootstrap and other variance estimators," *Commun Stat A-Theory* **38**(15), 2586–2603 (2009).